Fourier coupled-wave diffraction theory of periodic structures and crystals

Xian-Rong Huang,[1,*] Ru-Wen Peng,[2,†] Marcelo G. Hönnicke,[3] and Thomas Gog[1]
[1]*Advanced Photon Source, Argonne National Laboratory, Argonne, Illinois 60439, USA*
[2]*National Laboratory of Solid State Microstructures and Department of Physics, Nanjing University, Nanjing 210093, China*
[3]*Universidade Federal da Integração Latino-Americana, 85867-970 Foz do Iguaçu, PR, Brazil*
(Received 9 February 2013; published 18 June 2013)

The dynamical theory of x-ray diffraction and the coupled-wave theory for modeling diffraction of light from periodic structures are two equivalent theories but with incompatibilities, as they were developed independently along two parallel directions in history. Here we reformulate the two theories into a universal Fourier coupled-wave diffraction theory (FCWDT), in which the fundamental coupled-wave equations for almost all practical diffraction geometry can always be written as a straightforward eigenvalue equation that is easily solvable by standard mathematical procedures. Since it removes most of the approximations and complexities in the two conventional theories, the FCWDT is almost rigorous yet simple and, in principle, can be used to compute scattering of electromagnetic waves from any kinds of periodic (nonmagnetic) structures, including x-ray diffraction from crystals and soft x-ray and light diffraction from periodic multilayers, gratings, and photonic crystals.

DOI: 10.1103/PhysRevA.87.063828 PACS number(s): 42.25.Fx, 42.79.Dj, 61.05.cc, 42.70.Qs

I. INTRODUCTION

The *dynamical theory* is a well-established theory for modeling x-ray diffraction from single crystals [1,2]. In parallel, researchers have been developing the *coupled-wave theory* for computing diffraction of light from periodic photonic crystals (mainly planar gratings; see, e.g., [3–6]). In principle, the two theories are equivalent since they both treat the interactions of electromagnetic waves with periodical structures based on Fourier analyses of Maxwell's equations. The only major difference is that the interaction of short-wavelength x rays with crystals is a weak scattering process, compared to the usually strong scattering effect of long-wavelength light from periodically modulated media. Consequently, x-ray diffraction usually activates one or at most a few noticeable Bragg reflections simultaneously (called the two-beam and multiple-beam diffraction processes, respectively) [1,7,8], while light scattering from high-contrast photonic crystals may involve a large number of diffraction orders. Nevertheless, photonic crystal diffraction is largely equivalent to multiple-beam x-ray crystal diffraction, and it should be possible to model them with the same theory.

Unfortunately, the dynamical theory in history has adopted an unnecessarily different choice, i.e., the electric displacement **D** has been chosen as the basic variable for solving Maxwell's equations. This choice was based on the transversality condition $\nabla \cdot \mathbf{D} \equiv 0$ that can simplify Maxwell's equation. However, since the boundary conditions at the surfaces and interfaces are based on the continuity of the tangential components of the electric field **E** and the magnetic field **H**, in the dynamical theory one has to convert the **D** fields into **E** and **H** fields to solve the boundary equations [1,8], which is inconvenient and, at the same time, leads to a number of unnecessary approximations that may be valid only for weak scattering. Most significantly, these different formulas make the dynamical theory incompatible with the coupled-wave theory that is naturally based on **E** and **H** fields [4,5]. Due to these incompatibilities, it is not uncommon that many well-established x-ray diffraction mechanisms (including computational methods) are little known or have been "reinvented" with considerable efforts in the optical society, and vice versa.

The main purpose of this paper is to rewrite the dynamical theory and coupled-wave theory in a uniform yet simple format. We call the revised theory the *Fourier coupled-wave diffraction theory* (FCWDT), from which one will see that the fundamental principles and formulas of the two theories are indeed identical. Hence, the reformulated FCWDT not only bridges the two parallel fields so as to allow the sharing and exchanging of ideas with each other, but also provides a universal framework for modeling and computing diffraction of all kinds of electromagnetic waves from any periodic structures. Since it is derived solely from Maxwell's equations without assumptions, the FCWDT removes almost all of the approximations as well as most (extreme) complexities of both the conventional coupled-wave theory and dynamical theory. Therefore, it is rigorous and may have numerous applications for the design and development of the related optical devices.

This paper is mainly structured as follows. We start illustrating the FCWDT in Sec. II with the simplest case of coplanar two-beam diffraction for transverse-electric (TE) waves (together with the boundary conditions and the possible wave merging problem), followed by the treatments of general multiple-beam TE coplanar diffraction. In a similar way, we describe the FCWDT for coplanar diffraction of transverse-magnetic (TM) waves in Sec. III. Afterwards, the FCWDT treatments of general N-beam diffraction from three-dimensional (3D) periodic structures are given in Sec. IV.

II. COPLANAR DIFFRACTION FOR TE POLARIZATION

A. Two-beam asymmetric diffraction

We start by solving Maxwell's equations of monochromatic waves in nonmagnetic media (with the magnetic permeability

*xiahuang@aps.anl.gov
†rwpeng@nju.edu.cn

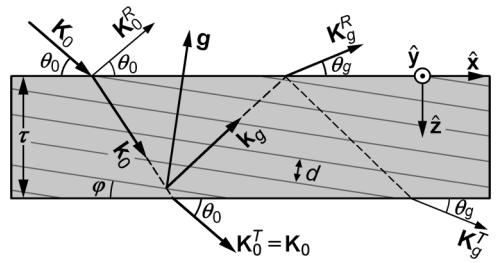

FIG. 1. Two-beam coplanar diffraction from a parallel-sided plate. $\hat{\mathbf{x}}$, $\hat{\mathbf{y}}$, and $\hat{\mathbf{z}}$ are unit vectors along the orthogonal x, y, and z axes, respectively.

$\mu \equiv 1$):

$$\nabla \times \mathbf{E} = -iK\mathbf{H}, \tag{1}$$

$$\nabla \times \mathbf{H} = iK\varepsilon\mathbf{E}, \tag{2}$$

where ε is the permittivity, $K = 2\pi/\lambda$, and λ is the wavelength in free space (in c.g.s. units). Consider two-beam diffraction (involving the incident beam and only one strong diffracted beam [1,2]) from a parallel (photonic) crystal plate of thickness τ in Fig. 1. Above the plate, the incident, specularly reflected and diffracted waves are $\tilde{\mathbf{E}}^I \exp(-i\mathbf{K}_0 \cdot \mathbf{r})$, $\tilde{\mathbf{E}}_0^R \exp(-i\mathbf{K}_0^R \cdot \mathbf{r})$, and $\tilde{\mathbf{E}}_g^R \exp(-i\mathbf{K}_g^R \cdot \mathbf{r})$, respectively. Below the plate exist a forward transmitted wave $\tilde{\mathbf{E}}_0^T \exp(-i\mathbf{K}_0^T \cdot \mathbf{r})$ and another diffracted wave $\tilde{\mathbf{E}}_g^T \exp(-i\mathbf{K}_g^T \cdot \mathbf{r})$. Inside the plate, there are a set of eigenmodes in the form $\mathbf{E}_0 \exp(-i\mathbf{k}_0 \cdot \mathbf{r}) + \mathbf{E}_g \exp(-i\mathbf{k}_g \cdot \mathbf{r})$, where $\mathbf{k}_g = \mathbf{k}_0 + \mathbf{g}$, and $\mathbf{g}$ is the diffraction vector. (Here we omit the common harmonic time factor of the waves.) Note that for the two-beam case, only one of the two diffracted waves $\tilde{\mathbf{E}}_g^{R,T}$ may have strong intensity, depending on the Bragg reflection or Laue transmission geometry [1,2].

Since coplanar diffraction is the most commonly used geometry, we first discuss this configuration in Fig. 1, where the diffraction vector $\mathbf{g}$ and all the wave vectors are parallel to the xz plane. In terms of the incidence angle θ_0, the incident wave vector is

$$\mathbf{K}_0 = K_{0x}\hat{\mathbf{x}} + K_{0z}\hat{\mathbf{z}} = K\cos\theta_0\,\hat{\mathbf{x}} + K\sin\theta_0\,\hat{\mathbf{z}}. \tag{3}$$

Accordingly, the specularly reflected wave vector is $\mathbf{K}_0^R = K_{0x}\hat{\mathbf{x}} - K_{0z}\hat{\mathbf{z}}$. Inside the plate, we may write $\mathbf{k}_0$ as

$$\mathbf{k}_0 = k_{0x}\hat{\mathbf{x}} + p\hat{\mathbf{z}}, \tag{4}$$

where $k_{0x} \equiv K_{0x}$ due to the continuity of the tangential wave-vector components across the surface. This also leads to $\mathbf{K}_0^T = \mathbf{K}_0$ (because $|\mathbf{K}_0^T| = K$). Similarly, since $\mathbf{k}_g$, $\mathbf{K}_g^R$, and $\mathbf{K}_g^T$ must have the same tangential component, we have

$$\begin{aligned} \mathbf{k}_g &= \mathbf{k}_0 + \mathbf{g} = k_{gx}\hat{\mathbf{x}} + (p + g_z)\hat{\mathbf{z}}, \\ k_{gx} &= K_{gx}^T = K_{gx}^R = k_{0x} + g_x. \end{aligned} \tag{5}$$

For elastic scattering, the vertical components of $\mathbf{K}_g^T$ and $\mathbf{K}_g^R$ are

$$K_{gz}^T = -K_{gz}^R = \begin{cases} \sqrt{\Delta_g} & \text{if } \Delta_g \geqslant 0 \\ -i\sqrt{-\Delta_g} & \text{otherwise,} \end{cases} \tag{6}$$

where $\Delta_g = K^2 - k_{gx}^2$. Here, if $\Delta_g < 0$, the external diffracted waves $\tilde{\mathbf{E}}_g^{R,T} \exp(-i\mathbf{K}_g^{R,T} \cdot \mathbf{r})$ become evanescent waves. The exit angle is $\theta_g = \cos^{-1}(k_{gx}/K)$ if $\Delta_g > 0$. (If there is a homogeneous substrate with permittivity $\varepsilon_s \neq 1$ below the bottom surface, K_{0z}^T and K_{gz}^T should be modified based on $|\mathbf{K}_{0,g}^T|^2 = \varepsilon_s K^2$.) Based on the known incident wave vector $\mathbf{K}_0$, we can thus determine all the external wave vectors and the tangential components of the internal wave vectors. The remaining task is to determine p and the wave amplitudes.

The TE-polarization waves (also called the σ-polarization waves in x-ray diffraction; $\mathbf{E} \| \hat{\mathbf{y}}$ in Fig. 1) satisfy $\nabla \cdot \mathbf{E} = 0$. Taking the curl of Eq. (1) and using Eq. (2) and $\nabla \cdot \mathbf{E} = 0$, we obtain

$$\nabla^2\mathbf{E}(\mathbf{r}) = -K^2\varepsilon(\mathbf{r})\mathbf{E}(\mathbf{r}). \tag{7}$$

This is the equation that needs to be solved. For a periodic structure, the periodically modulated permittivity $\varepsilon(\mathbf{r})$ can be expanded as a Fourier series,

$$\varepsilon(\mathbf{r}) = \sum \epsilon_m \exp(-i\mathbf{g}_m \cdot \mathbf{r}), \tag{8}$$

with

$$\epsilon_m = \Omega^{-1} \int_\Omega \varepsilon(\mathbf{r}) \exp(i\mathbf{g}_m \cdot \mathbf{r}) d\mathbf{r} \tag{9}$$

for general photonic crystals, where Ω is the volume of the unit cell and $\mathbf{g}_m$ is any reciprocal lattice vector. For the specific cases of x-ray diffraction, the crystal susceptibility is $\chi = \varepsilon - 1$, which leads to $\epsilon_m = \chi_m$ for $m \neq 0$ and $\epsilon_0 = 1 + \chi_0$. Here the χ_m's (proportional to the structure factors) are the Fourier coefficients of χ used in the dynamical theory [1,2]. For periodic multilayers and one-dimensional (1D) gratings, $\epsilon_m = (1/d)\int_0^d \varepsilon(Z)\exp(ig_m Z)dZ$, where d is the period of the structure, $g_m = 2\pi m/d$ (with m being the diffraction order), and the Z axis is perpendicular to the layers [9]. The TE electric field in the plate can also be expanded as a plane-wave series,

$$\mathbf{E}(\mathbf{r}) = \hat{\mathbf{y}} \sum E_m \exp(-i\mathbf{k}_m \cdot \mathbf{r}), \tag{10}$$

where $\mathbf{k}_m = \mathbf{k}_0 + \mathbf{g}_m$. Inserting Eqs. (8) and (10) into Eq. (7) yields the general *coupled-wave equations* for TE polarization:

$$k_m^2 E_m = K^2 \sum_n \epsilon_{m-n} E_n. \tag{11}$$

For the two-beam case in Fig. 1 with only one diffraction vector $\mathbf{g}$, Eq. (11) reduces to

$$k_0^2 E_0 = K^2\epsilon_0 E_0 + K^2\epsilon_{\overline{g}} E_g, \tag{12}$$

$$k_g^2 E_g = K^2\epsilon_g E_0 + K^2\epsilon_0 E_g, \tag{13}$$

where $\overline{g} = -g$. Equations (12) and (13) can be treated as an eigenvalue system (see Sec. II C), but here, for readers familiar with the conventional x-ray dynamical theory, we directly solve their secular equation (also called the dispersion-surface equation [1,2])

$$\left(K^2\epsilon_0 - k_0^2\right)\left(K^2\epsilon_0 - k_g^2\right) = K^4\epsilon_g\epsilon_{\overline{g}}. \tag{14}$$

Based on Eqs. (4) and (5), this equation can be written as

$$p^4 + 2g_z p^3 + a_2 p^2 + 2g_z a_1 p + a_0 = 0, \tag{15}$$

where $a_0 = k_{0x}^2(B - k_{0x}^2) - K^2 B\epsilon_0 + K^4(\epsilon_0^2 - \epsilon_g\epsilon_{\overline{g}})$, $a_1 = k_{0x}^2 - K^2\epsilon_0$, $a_2 = B - 2K^2\epsilon_0$, and $B = k_{0x}^2 + k_{gx}^2 + g_z^2$. Equation (15) has four complex roots p_ι ($\iota = 1,2,3,4$) that may

be analytically solved [10]. Here we sort the four roots such that $\mathrm{Im}(p_{1,2}) < 0$ and $\mathrm{Im}(p_{3,4}) > 0$. Each root corresponds to an eigenmode $E_0^{(\iota)}\hat{\mathbf{y}}[\exp(-i\mathbf{k}_0^{(\iota)}\cdot\mathbf{r}) + r_\iota \exp(-i\mathbf{k}_g^{(\iota)}\cdot\mathbf{r})]$ in the plate, where $\mathbf{k}_0^{(\iota)} = k_{0x}\hat{\mathbf{x}} + p_\iota\hat{\mathbf{z}}$ and $\mathbf{k}_g^{(\iota)} = k_{gx}\hat{\mathbf{x}} + k_{gz}^{(\iota)}\hat{\mathbf{z}}$ with $k_{gz}^{(\iota)} = p_\iota + g_z$. Meanwhile, the wave amplitude ratio is determined by $r_\iota = E_g^{(\iota)}/E_0^{(\iota)} = [-\epsilon_0 + (k_0^{(\iota)})^2/K^2]/\epsilon_{\bar{g}}$ according to Eq. (12).

According to Eq. (1), the magnetic field of a plane wave $\mathbf{E}\exp(-i\mathbf{k}\cdot\mathbf{r})$ is simply $\mathbf{H}\exp(-i\mathbf{k}\cdot\mathbf{r})$, with $\mathbf{H} = \mathbf{k}\times\mathbf{E}/K$. Then, based on the calculated p_ι, $k_{gz}^{(\iota)}$, and r_ι, the tangential magnetic amplitudes of each eigenmode in the crystal can be derived as $H_{0x}^{(\iota)} = -s_0^{(\iota)}E_0^{(\iota)}/K$ and $H_{gx}^{(\iota)} = -s_g^{(\iota)}E_0^{(\iota)}/K$, where $s_0^{(\iota)} = p_\iota$ and $s_g^{(\iota)} = r_\iota k_{gz}^{(\iota)}$. Hence, the continuity of the tangential electric and magnetic fields across the two surfaces in Fig. 1 gives

$$\begin{aligned}
\tilde{E}^I + \tilde{E}_0^R &= \textstyle\sum E_0^{(\iota)}, \quad K_{0z}\big(\tilde{E}^I - \tilde{E}_0^R\big) = \textstyle\sum s_0^{(\iota)}E_0^{(\iota)},\\
\tilde{E}_g^R &= \textstyle\sum r_\iota E_0^{(\iota)}, \quad -K_{gz}^T\tilde{E}_g^R = \textstyle\sum s_g^{(\iota)}E_0^{(\iota)},\\
\Phi_0\tilde{E}_0^T &= \textstyle\sum \phi_0^{(\iota)}E_0^{(\iota)}, \quad K_{0z}\Phi_0\tilde{E}_0^T = \textstyle\sum s_0^{(\iota)}\phi_0^{(\iota)}E_0^{(\iota)},\\
\Phi_g\tilde{E}_g^T &= \textstyle\sum r_\iota\phi_g^{(\iota)}E_0^{(\iota)}, \quad K_{gz}^T\Phi_g\tilde{E}_g^T = \textstyle\sum s_g^{(\iota)}\phi_g^{(\iota)}E_0^{(\iota)},
\end{aligned} \tag{16}$$

where all the summations are over $\iota = 1,2,3,4$, $\phi_0^{(\iota)} = \exp(-ip_\iota\tau)$, $\phi_g^{(\iota)} = \phi_0^{(\iota)}\exp(-ig_z\tau)$, $\Phi_0 = \exp(-iK_{0z}\tau)$, and $\Phi_g = \exp(-iK_{gz}^T\tau)$. For thick lossy (absorbing) structures, $\phi_0^{(3)}$ and $\phi_0^{(4)}$ may cause numerical inaccuracy or overflow. To avoid this problem, one may replace $\phi_0^{(\iota)}E_0^{(\iota)}$ with $\mathcal{E}_0^{(\iota)}$ in the last four equations and replace $E_0^{(\iota)}$ with $\mathcal{E}_0^{(\iota)}\exp(ip_\iota\tau)$ in the first four equations for $\iota = 3,4$ to change Eqs. (16) into equations about eight unknowns, $\tilde{E}_0^R$, $\tilde{E}_g^R$, $\tilde{E}_g^R$, $\tilde{E}_g^T$, $E_0^{(1)}$, $E_0^{(2)}$, $\mathcal{E}_0^{(3)}$, and $\mathcal{E}_0^{(4)}$ [11]. Here, $\mathcal{E}_0^{(3)}$ and $\mathcal{E}_0^{(4)}$ are the wave amplitudes at the bottom surface. For lossy structures, such treatments are almost always necessary to avoid numerical instability (for all the following cases).

After Eqs. (16) are solved, the two diffraction efficiency values are $R_g = |b||\tilde{E}_g^R/\tilde{E}^I|^2$ and $T_g = |b||\tilde{E}_g^T/\tilde{E}^I|^2$ (for $\Delta_g > 0$), where $|b| = K_{gz}^T/K_{0z}$ is the asymmetry factor. The specular reflectivity is $R_0 = |\tilde{E}_0^R/\tilde{E}^I|^2$ and the forward transmissivity is $T_0 = |\tilde{E}_0^T/\tilde{E}^I|^2$. These formulas are valid for both Bragg reflection and Laue transmission cases. For the Bragg case of a semi-infinite lossy plate ($\tau\to\infty$), the eigenmodes $\iota = 3,4$ may be ignored, and one can calculate R_g and R_0 from the first four equations of Eqs. (16) [11].

For x-ray diffraction from single crystals, the above simple FCWDT gives exactly the same results as the method described in [10] for any TE coplanar two-beam diffraction, including grazing-incidence and grazing-exit diffraction and backward diffraction (with the Bragg angle $\theta_B \simeq 90^\circ$). The advantage of this method is that it is only based on the **E** and **H** fields without the complication of the **D** fields and the associated approximations. Therefore, this method is within the framework of the coupled-wave theory for general optics and can be seamlessly extended also for modeling diffraction from periodic multilayers, gratings, and photonic crystals.

B. Symmetric Bragg reflection

In fact, from the extensive studies in the literature, the coupled-wave theory, which is consistent with the above FCWDT, has been demonstrated to be accurate for 1D gratings (e.g., see [12] and the supplemental material). The other way to theoretically prove the FCWDT is to compare it with Parratt's method [13] (or the transfer-matrix method [14]) for on-axis periodic multilayer structures.

As shown in Fig. 2(a), we consider a binary periodic multilayer with the refractive indices of the two sublayers being n_a and n_b, respectively. We study the weak-contrast condition $|\Delta n| \ll \bar{n} = (n_a + n_b)/2$, where $\Delta n = n_a - n_b$. In Fig. 2(c), the solid curve R_P is the reflectivity calculated by Parratt's recursion method [13] in the entire angular range $0 < \theta_0 \leqslant 90^\circ$. For most of the incidence angles θ_0, the multilayer acts as a homogeneous etalon with an average refractive index $\bar{n}$, so most of the fringes are due to the interference between the waves specularly reflected from the upper and lower surfaces (see [14], p. 360). But near the Bragg angle $\theta_B = 57.4^\circ$, strong diffraction occurs. Here, with the strong refraction effect taken into account, the Bragg equation is $2d(\bar{n}^2 - \cos^2\theta_B)^{1/2} = \lambda$.

To use the FCWDT to calculate the reflectivity, one immediately encounters a problem. The above FCWDT considers the specularly reflected wave $\tilde{E}_0^R$ and the Bragg diffracted wave $\tilde{E}_g^R$ separately, which yields two reflectivity values R_0 and R_g. However, for the symmetric reflection in Fig. 2(a) (with $g_x = 0$), $\tilde{E}_0^R$ and $\tilde{E}_g^R$ merge into a single plane wave due to $\mathbf{K}_0^R \equiv \mathbf{K}_g^R$ (and the $\tilde{E}_g^T$ and $\tilde{E}_0^T$ waves also merge together). Then which reflectivity value in the FCWDT corresponds to R_P for the symmetric case?

Figure 2(b) shows the specular reflectivity R_0 and the Bragg reflectivity R_g calculated by the FCWDT with the boundary conditions of Eqs. (16). Near the Bragg peak, R_0 and R_g both deviate significantly from R_P. Here one may wonder if the combined reflectivity is $R_0 + R_g$ [3], but the $R_0 + R_g$ curve in Fig. 2(b) still noticeably differs from R_P. [We have also tried to calculate the reflectivity using $R = |\tilde{E}_0^R + \tilde{E}_g^R|^2/|\tilde{E}^I|^2$, but this is obviously incorrect since R may exceed unity (not shown).]

The correct way to solve this problem is to merge $\tilde{E}_g^R$ ($\tilde{E}_g^T$) into $\tilde{E}_0^R$ ($\tilde{E}_0^T$) in the boundary equations (16). Then, Eqs. (16) for the symmetric case become

$$\begin{aligned}
\tilde{E}^I + \tilde{E}_0^R &= \textstyle\sum(1 + r_\iota)E_0^{(\iota)},\\
K_{0z}\big(\tilde{E}^I - \tilde{E}_0^R\big) &= \textstyle\sum\big(s_0^{(\iota)} + s_g^{(\iota)}\big)E_0^{(\iota)},\\
\Phi_g\tilde{E}_0^T &= \textstyle\sum\big(\phi_0^{(\iota)} + r_\iota\phi_g^{(\iota)}\big)E_0^{(\iota)},\\
K_{0z}\Phi_g\tilde{E}_0^T &= \textstyle\sum\big(s_0^{(\iota)}\phi_0^{(\iota)} + s_g^{(\iota)}\phi_g^{(\iota)}\big)E_0^{(\iota)}.
\end{aligned} \tag{17}$$

However, Eqs. (17) can contain only four unknowns, while we have six unknowns, $\tilde{E}_0^R$, $\tilde{E}_0^T$, and $E_0^{(\iota)}$ ($\iota = 1,2,3,4$), to solve. To overcome this difficulty, we rearrange the four roots of Eq. (15) in the order $\mathrm{Re}(p_3) < \mathrm{Re}(p_{1,2}) < \mathrm{Re}(p_4)$. Afterwards, it can be proved that $\mathbf{k}_0^{(1)}$ and $\mathbf{k}_0^{(2)}$ are very close to $\bar{\mathbf{k}}_0$, where $\bar{\mathbf{k}}_0$ is the average refracted wave vector in a homogenous plate with refractive index $\bar{n}$. This indicates that the corresponding eigenmodes $E_0^{(\iota)}\exp(-i\mathbf{k}_0^{(\iota)}\cdot\mathbf{r}) + E_g^{(\iota)}\exp(-i\mathbf{k}_g^{(\iota)}\cdot\mathbf{r})$ (for $\iota = 1,2$) are the two regular eigenmodes treated in the classical dynamical theory [1,2].

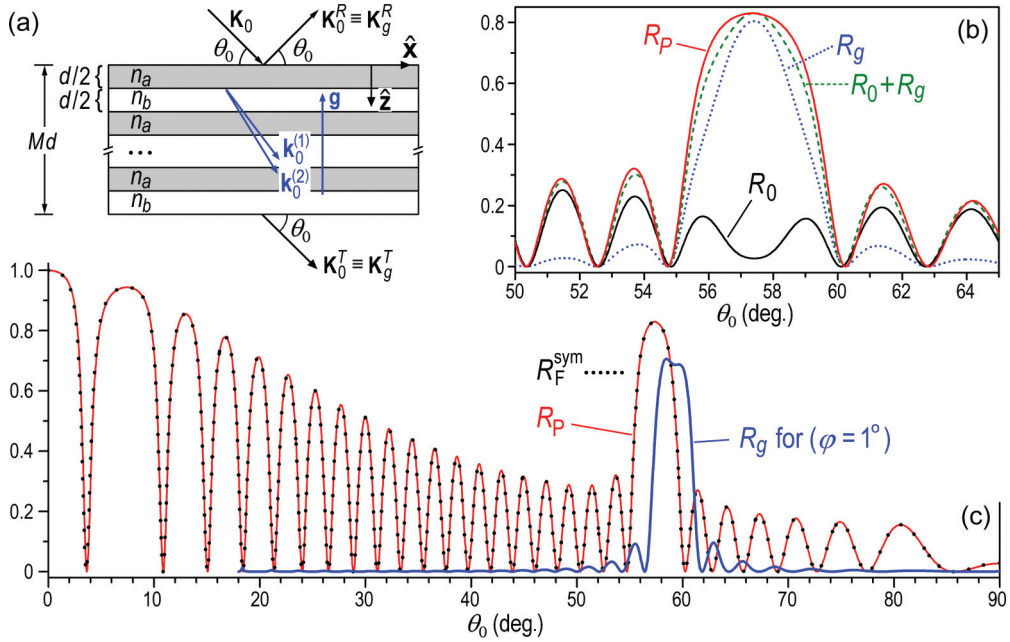

FIG. 2. (Color online) (a) Schematic of symmetric Bragg reflection from a periodic binary multilayer. (b) Comparison of the Parratt reflectivity (R_P) with the three reflectivity curves calculated from the FCWDT with the four-eigenmode boundary conditions of Eqs. (16). (c) Comparison of R_P with the reflectivity calculated from the two-eigenmode boundary conditions of Eqs. (17). $n_a = 1.51$, $n_b = 1.49$, $M = 100$, and the incident wavelength is always $\lambda = 1.12d$. TE polarization of two-beam coplanar diffraction.

The third eigenmode has the properties $r_3 = E_g^{(3)}/E_0^{(3)} \simeq 0$ (corresponding to $E_g^{(3)} \simeq 0$) and $\mathbf{k}_0^{(3)} \simeq \bar{\mathbf{k}}_0 + \mathbf{g}$, i.e., this eigenmode virtually has only one wave $E_0^{(3)} \exp(-i\mathbf{k}_0^{(3)} \cdot \mathbf{r})$, which represents internal specular reflection of waves $E_0^{(1,2)} \exp(-i\mathbf{k}_0^{(1,2)} \cdot \mathbf{r})$ from the bottom surface. For the symmetric case in Fig. 2(a), $E_0^{(3)} \exp(-i\mathbf{k}_0^{(3)} \cdot \mathbf{r})$ in fact merges into the two diffracted waves, $E_g^{(1,2)} \exp(-i\mathbf{k}_g^{(1,2)} \cdot \mathbf{r})$. Therefore, the third eigenmode must be removed from Eqs. (17). Similarly, the fourth eigenmode has the properties $E_0^{(4)} \simeq 0$ (since $|r_4| \gg 1$) and $\mathbf{k}_g^{(4)} \simeq \bar{\mathbf{k}}_0$, and the remaining wave $E_g^{(4)} \exp(-i\mathbf{k}_g^{(4)} \cdot \mathbf{r})$ represents internal specular reflection of waves $E_g^{(1,2)} \exp(-i\mathbf{k}_0^{(1,2)} \cdot \mathbf{r})$ from the top surface. For the symmetric geometry, since $E_g^{(4)} \exp(-i\mathbf{k}_g^{(4)} \cdot \mathbf{r})$ merges into waves $E_0^{(1,2)} \exp(-i\mathbf{k}_0^{(1,2)} \cdot \mathbf{r})$, the fourth eigenmode should also be removed from Eqs. (17).

Equations (17) now have only four unknowns, $\tilde{E}_0^R$, $\tilde{E}_0^T$, $E_0^{(1)}$, and $E_0^{(2)}$ (i.e., all the summations are over $\iota = 1,2$), that can be solved. The dotted line in Fig. 2(c) shows the reflectivity $R_F^{sym} = |\tilde{E}_0^R/\tilde{E}^I|^2$ calculated from Eqs. (17) with the two eigenmodes $\iota = 1,2$. Surprisingly, R_F^{sym} almost perfectly agrees with R_P in the entire range $0 < \theta_0 < 90°$, which clearly demonstrates the validity of the FCWDT even when Bragg diffraction is mixed with strong specular reflection. In addition to the large refractive index $\bar{n} = 1.5$ (compared with $|\bar{n} - 1| \sim 10^{-4}$ for hard x-ray diffraction), the refractive index contrast $\Delta n = 0.02$ in Fig. 2 is also much larger than that for x-ray diffraction ($\Delta n \sim 10^{-5}$). We have chosen these parameters in order to demonstrate that the FCWDT is applicable not only to x-ray diffraction, but also to light (and soft x-ray) diffraction from multilayers and photonic crystals.

To our knowledge, the wave merging (degeneration) problem has been overlooked in the literature. However, it may be unavoidable in 2D or 3D photonic crystal diffraction involving both symmetric and asymmetric diffraction vectors simultaneously (see Fig. 3), where Parratt's method is inapplicable. In fact, for 2D and 3D diffraction, wave merging occurs whenever two of the involved diffraction vectors have the same tangential components (with respect to the plate surfaces). Here we have illustrated some clues about how to overcome this difficulty.

For asymmetric diffraction, since the diffracted waves are separated from the specularly reflected (and forward refracted and/or transmitted) waves both inside and outside the plate, the boundary conditions of Eqs. (16) are rigorous for two-beam diffraction. As an example, Fig. 2(c) also shows the Bragg reflectivity curve R_g calculated with Eqs. (16) under the condition that the multilayer structure in Fig. 2(a) is offcut by an angle $\varphi = 1°$ (see Fig. 1). Without the mixing of specular reflection, the Bragg diffraction here gives a well-defined Bragg peak with much cleaner background compared with that for the symmetric case $\varphi = 0$. This is one of the

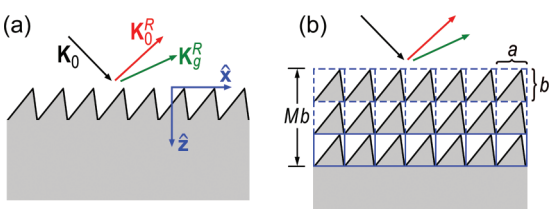

FIG. 3. (Color online) The treatment of the nonplanar grating (a) as a 2D photonic crystal (b) but with a thickness $M = 1$ in the FCWDT. The surface profile of the unit cell can be of arbitrary shape. a and b are the lattice constants.

many advantages of (dispersive) asymmetric multilayers or gratings [9].

Note that for symmetric x-ray crystal diffraction, Eqs. (17) and (16) lead to virtually the same results because x-ray specular reflection is negligible in nongrazing geometry. Thus, for x-ray diffraction, one may almost always use Eqs. (16) without the necessity to differentiate symmetric and asymmetric configurations. For multilayer diffraction, however, it is safer to use Eqs. (17) (or simply Parratt's method) for symmetric reflection.

C. *N*-beam coplanar diffraction of TE polarization

If the periodic structure has high contrast Δn, retaining higher diffraction orders in the FCWDT may become necessary. For the coplanar diffraction geometry, extension of the above FCWDT to the N-beam cases is convenient. In Fig. 1, consider the situation that N diffraction orders are retained with the diffraction vectors all parallel to the xz plane. We write them as $\mathbf{g}_0, \mathbf{g}_1, \ldots, \mathbf{g}_{N-1}$, where $\mathbf{g}_0 = \mathbf{0}$ and $N > 1$. Based on Eq. (4), each internal diffracted vector can be written as $\mathbf{k}_m = (k_{0x} + g_{mx})\hat{\mathbf{x}} + (p + g_{mz})\hat{\mathbf{z}}$, which leads to

$$k_m^2 = (k_{0x} + g_{mx})^2 + g_{mz}^2 + 2g_{mz}p + p^2. \tag{18}$$

Based on this equation, Eqs. (11) can be written as an eigenvalue equation:

$$(p^2\boldsymbol{I} - p\boldsymbol{V}^\sigma + \boldsymbol{U}^\sigma)\underline{\mathbf{E}} = \mathbf{0}, \tag{19}$$

where $\underline{\mathbf{E}} = (E_0, E_1, \ldots, E_{N-1})^T$ is a column vector about the internal wave amplitudes, $\boldsymbol{I}$ is the $N \times N$ identity matrix, $\boldsymbol{V}^\sigma$ is a diagonal matrix with $V^\sigma_{m,m} = -2g_{mz}$, and $\boldsymbol{U}^\sigma$ is a matrix with off-diagonal elements $U^\sigma_{m,n} = -K^2\epsilon_{m-n}$ (for $m \neq n$) and diagonal elements $U^\sigma_{m,m} = (k_{0x} + g_{mx})^2 + g_{mz}^2 - K^2\epsilon_0$. Here the indices (m,n) of the matrix elements are also from 0 to $N-1$, and all the elements are known. Equation (19) now has the same form as Eq. (10) in Ref. [7]. So one can use the simple and elegant method in the appendix of [7] to obtain $2N$ eigenvalues p_ι and the corresponding $2N$ eigenvectors $\underline{\mathbf{E}}^{(\iota)}$ ($\iota = 1,2,\ldots,2N$), i.e., the eigenvalues p_ι of Eq. (19) are actually the eigenvalues of the $2N \times 2N$ eigenequation

$$\begin{pmatrix} \boldsymbol{V}^\sigma & -\boldsymbol{U}^\sigma \\ \boldsymbol{I} & \boldsymbol{O} \end{pmatrix} \mathbf{X} = p\mathbf{X}, \tag{20}$$

where $\boldsymbol{O}$ is the $N \times N$ null matrix, and $\mathbf{X}$ is a column vector with $2N$ elements. The elements of each eigenvector $\underline{\mathbf{E}}^{(\iota)}$ for Eq. (19) are the first N elements of the corresponding eigenvector $\mathbf{X}^{(\iota)}$ obtained from Eq. (20).

Meanwhile, each diffraction vector $\mathbf{g}_m$ induces a diffracted wave $\tilde{E}_m^R \exp(-\mathbf{K}_m^R \cdot \mathbf{r})$ above the plate and another diffracted wave $\tilde{E}_m^T \exp(-\mathbf{K}_m^T \cdot \mathbf{r})$ below the plate in Fig. 1, where $\mathbf{K}_m^R$ and $\mathbf{K}_m^T$ can be obtained from Eqs. (5) and (6) with the corresponding $\mathbf{g}_m$. For the asymmetric geometry in Fig. 1, the boundary conditions about the continuity of the tangential $\mathbf{E}$ and $\mathbf{H}$ fields at the upper and lower surfaces can be written as $4N$ linear equations about the unknowns $\tilde{E}_m^R, \tilde{E}_m^T, E_0^{(\iota)}$ (for $m = 0,1,\ldots,N-1$ and $\iota = 1,2,\ldots,2N$), and their solutions then determine all the diffraction properties. However, if any two diffraction vectors have the same x components ($g_{mx} = g_{nx}$ for $m \neq n$), then some of the associated waves merge together. Therefore, the corresponding eigenmodes should be removed from the boundary equations. Particularly for the symmetric configuration of periodic multilayers ($\varphi = 0$, so $g_{mx} \equiv 0$), the $2N$ eigenvectors from Eq. (19) always degenerate into only two eigenvectors due to $\mathbf{K}_0^R = \mathbf{K}_1^R = \cdots = \mathbf{K}_{N-1}^R$ and $\mathbf{K}_0^T = \mathbf{K}_1^T = \cdots = \mathbf{K}_{N-1}^T$, similar to the above two-beam case. Consequently, the boundary conditions reduce to four linear equations about $\tilde{E}_0^R$, $\tilde{E}_0^T$, $E_0^{(1)}$, and $E_0^{(2)}$, similar to Eqs. (17).

Note that for a 1D periodic grating with the lattice planes perpendicular to the surfaces in Fig. 1 ($\varphi = 90^\circ$), we have $g_{mz} \equiv 0$ and $\boldsymbol{V}^\sigma = \boldsymbol{O}$. Then, Eq. (19) reduces to a standard eigenvalue equation

$$(p^2\boldsymbol{I} + \boldsymbol{U}^\sigma)\underline{\mathbf{E}} = \mathbf{0} \tag{21}$$

in terms of p^2. This simpler case has been well studied in the literature (see [4] for details as well as the boundary equations). However, Eq. (19) is more general since it is also valid and accurate for TE-polarization diffraction from any oblique periodic gratings and multilayers (even with extremely high contrast), except that the surfaces must be flat (i.e., planar gratings). Moreover, Eq. (19) only requires that all the $\mathbf{g}_m$ vectors be parallel to the xz plane in Fig. 1, but not necessarily parallel to each other (see [15] for such a case of TE coplanar multiple-beam x-ray diffraction).

In the literature, the coupled-wave theory was developed mainly for 1D planar periodic structures, but here Eq. (19) can also be used to compute diffraction of slanted gratings [16] and in-plane scattering of 2D photonic crystals. For example, the nonplanar surface-relief grating [17,18] in Fig. 3(a) may be treated as a 2D photonic crystal in Fig. 3(b). In this case, the eigenequation of Eq. (19) must also include the diffraction vectors that have z components. After the eigenmodes of the 2D system are solved, one can set the thickness of the 2D crystal back to $\tau = b$ ($M = 1$) in the boundary equations to obtain the diffraction properties of the original grating. Compared with the complicated conventional treatments in which the arbitrary-profile grating is usually approximated by a stack of thin laminae ([18,19] and references therein), the treatment in Fig. 3 is simpler and more accurate without suffering from absorption-induced numerical overflow or instability in the boundary equations. The convergence speed may also be much faster.

III. TM POLARIZATION

A. Two-beam coplanar diffraction

Except for TE coplanar diffraction, generally $\nabla \cdot \mathbf{E} \neq 0$ in inhomogeneous media, which makes Eq. (7) invalid. Fortunately, we have the universal transversality condition of the magnetic field: $\nabla \cdot \mathbf{H} \equiv 0$. Now we rewrite Eq. (2) as $\varepsilon^{-1}\nabla \times \mathbf{H} = iK\mathbf{E}$. Taking the curl of this equation and using Eq. (1), we obtain

$$\nabla \times [\varepsilon^{-1}(\mathbf{r})\nabla \times \mathbf{H}(\mathbf{r})] = K^2\mathbf{H}(\mathbf{r}), \tag{22}$$

which is always valid (including TE polarization). For coplanar diffraction of TM polarization (also called π polarization in x-ray diffraction) in Fig. 1, the magnetic field in the plate can be written as

$$\mathbf{H}(\mathbf{r}) = \hat{\mathbf{y}} \sum H_m \exp(-i\mathbf{k}_m \cdot \mathbf{r}). \tag{23}$$

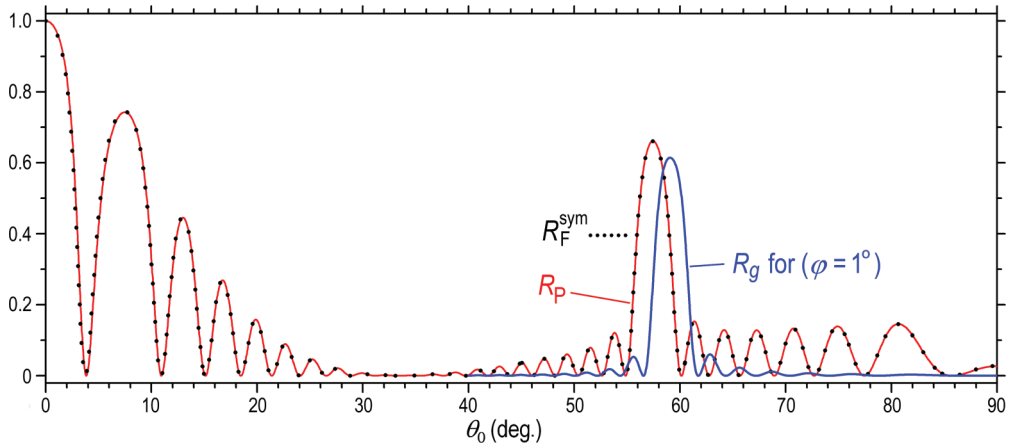

FIG. 4. (Color online) Repeated calculations of the Parratt reflectivity (R_P) and the FCWDT Bragg reflectivity based on the diffraction configuration and parameters of Fig. 2(c) but for TM polarization of two-beam coplanar diffraction.

Meanwhile, the Fourier expansion of ε^{-1} is

$$\varepsilon^{-1}(\mathbf{r}) = \sum \zeta_m \exp(-i\mathbf{g}_m \cdot \mathbf{r}). \tag{24}$$

Compared with Eq. (9), here

$$\zeta_m = \Omega^{-1} \int_\Omega \frac{1}{\varepsilon(\mathbf{r})} \exp(i\mathbf{g}_m \cdot \mathbf{r}) d\mathbf{r}. \tag{25}$$

For x-ray diffraction from crystals, $\varepsilon^{-1} = (1+\chi)^{-1} \simeq 1 - \chi$ gives $\zeta_m = -\chi_m$ for $m \neq 0$ and $\zeta_0 = 1 - \chi_0$. Inserting Eqs. (23) and (24) into Eq. (22), we obtain the coupled-wave equations for TM polarization:

$$K^2 H_m = \sum_n \zeta_{m-n}(\mathbf{k}_m \cdot \mathbf{k}_n) H_n. \tag{26}$$

For the two-beam coplanar case in Fig. 1 with $\mathbf{H} \| \hat{\mathbf{y}}$, we write the external waves as $\tilde{H}^I \exp(-i\mathbf{K}_0 \cdot \mathbf{r})$, $\tilde{H}_0^R \exp(-i\mathbf{K}_0^R \cdot \mathbf{r})$, $\tilde{H}_g^R \exp(-i\mathbf{K}_g^R \cdot \mathbf{r})$, $\tilde{H}_0^T \exp(-i\mathbf{K}_0 \cdot \mathbf{r})$, and $\tilde{H}_g^T \exp(-i\mathbf{K}_g^T \cdot \mathbf{r})$. The internal waves are $H_0 \exp(-i\mathbf{k}_0 \cdot \mathbf{r})$ and $H_g \exp(-i\mathbf{k}_g \cdot \mathbf{r})$. Now, Eqs. (26) reduce to

$$K^2 H_0 = \zeta_0 k_0^2 H_0 + \zeta_{\bar{g}}(\mathbf{k}_0 \cdot \mathbf{k}_g) H_g, \tag{27}$$

$$K^2 H_g = \zeta_g(\mathbf{k}_0 \cdot \mathbf{k}_g) H_0 + \zeta_0 k_g^2 H_g. \tag{28}$$

The secular equation of Eqs. (27) and (28) is

$$\left(\zeta_0 k_0^2 - K^2\right)\left(\zeta_0 k_g^2 - K^2\right) = \zeta_g \zeta_{\bar{g}} (\mathbf{k}_0 \cdot \mathbf{k}_g)^2, \tag{29}$$

which can also be written in the form of Eq. (15), but the coefficients become $a_0 = [\zeta_0^2 k_{0x}^2 (B - k_{0x}^2) - K^2 B \zeta_0 + K^4 - \zeta_g \zeta_{\bar{g}} k_{0x}^2 k_{gx}^2]/C$, $a_1 = (k_{0x}^2 \zeta_0^2 - K^2 \zeta_0 - \zeta_g \zeta_{\bar{g}} k_{0x} k_{gx})/C$, $a_2 = [B\zeta_0^2 - 2K^2\zeta_0 - \zeta_g \zeta_{\bar{g}}(2k_{0x}k_{gx} + g_z^2)]/C$, $B = k_{0x}^2 + k_{gx}^2 + g_z^2$, and $C = \zeta_0^2 - \zeta_g \zeta_{\bar{g}}$ for TM polarization. Similarly, we can obtain four complex roots p_ι from Eq. (15). Each root corresponds to an eigenmode $H_0^{(\iota)}[\exp(-i\mathbf{k}_0^{(\iota)} \cdot \mathbf{r}) + r_\iota \exp(-i\mathbf{k}_g^{(\iota)} \cdot \mathbf{r})]\hat{\mathbf{y}}$ in the plate with the amplitude ratio being $r_\iota = H_g^{(\iota)}/H_0^{(\iota)} = [K^2 - (k_0^{(\iota)})^2 \zeta_0]/[\zeta_{\bar{g}}(K_{0x}k_{gx} + p_\iota k_{gz}^{(\iota)})]$ according to Eq. (27).

In order to use the boundary conditions, we have to derive the $\mathbf{E}$ field of each $\mathbf{H}$ wave. For the external waves (satisfying $\varepsilon = 1$ and $\mathbf{K} \cdot \tilde{\mathbf{E}} = 0$), we have $\tilde{\mathbf{E}} = -\mathbf{K} \times \tilde{\mathbf{H}}$ according to either Eq. (1) or Eq. (2), where $\mathbf{K}$ is the wave vector of the external $\tilde{\mathbf{H}}$ wave. But as mentioned above, $\nabla \cdot \mathbf{E} \neq 0$ inside the plate. So the conversion of the internal fields $\mathbf{H}$ to $\mathbf{E}$ must use the Fourier transformation of Eq. (2),

$$\mathbf{E}_m^{(\iota)} = -\frac{1}{K} \sum_n \zeta_{m-n} \mathbf{k}_n^{(\iota)} \times \mathbf{H}_n^{(\iota)}. \tag{30}$$

This equation indicates that $\mathbf{E}_m^{(\iota)}$ not only depends on $\mathbf{H}_m^{(\iota)}$, but is also related to all the other amplitudes in the eigenmode. Applying Eq. (30), one may prove that for the two-beam TM-polarization case, the tangential components of the internal $\mathbf{E}$ amplitudes can be written as $E_{0x}^{(\iota)} = s_0^{(\iota)} H_0^{(\iota)}/K$ and $E_{gx}^{(\iota)} = s_g^{(\iota)} H_0^{(\iota)}/K$ with $s_0^{(\iota)} = \zeta_0 p_\iota + \zeta_{\bar{g}} k_{gz}^{(\iota)} r_\iota$ and $s_g^{(\iota)} = \zeta_g p_\iota + \zeta_0 k_{gz}^{(\iota)} r_\iota$. Afterwards, the boundary conditions for TM polarization have the same forms as Eqs. (16) or (17) except that the E and $\tilde{E}$ amplitudes in Eqs. (16) or (17) are replaced by the H and $\tilde{H}$ amplitudes, respectively. Meanwhile, the parameters p_ι, $k_{gz}^{(\iota)}$, r_ι, $s_0^{(\iota)}$, and $s_g^{(\iota)}$ in Eqs. (16) or (17) should adopt the current values for TM polarization. After the boundary equations are solved, we obtain $R_0 = |\tilde{H}_0^R/\tilde{H}^I|^2$, $R_g = |b||\tilde{H}_g^R/\tilde{H}^I|^2$, $T_0 = |\tilde{H}_0^T/\tilde{H}^I|^2$, and $T_g = |b||\tilde{H}_g^T/\tilde{H}^I|^2$ with $|b| = K_{gz}^T/K_{0z}$. For x-ray diffraction from crystals, we have tested that these formulas give exactly the same results as the method described in [20].

Based on the same parameters in Fig. 2(c), we have repeated the calculations of the Parratt reflectivity R_P and the FCWDT reflectivity R_F^{sym} in Fig. 4 for symmetric TM-polarization reflection. Again R_F^{sym} almost perfectly agrees with R_P in the entire angular range $0 < \theta_0 < 90°$. Here the suppression of specular reflection around $\theta_0 = 34°$ is due to $\bar{\mathbf{k}}_0 \cdot (\bar{\mathbf{k}}_0 + \mathbf{g}) \simeq 0$, where $\bar{\mathbf{k}}_0 \cdot (\bar{\mathbf{k}}_0 + \mathbf{g})$ is equivalent to the TM-polarization factor used in the classical dynamical theory [1,2]. The R_g curve for asymmetric diffraction ($\varphi = 1°$) in Fig. 4 shows a Bragg peak surrounded by slight fringes due to the finite plate thickness, similar to that in Fig. 2(c).

B. *N*-beam coplanar diffraction of TM polarization

The above two-beam TM coplanar diffraction formulation can also be extended to the N-beam case for diffraction of

high-contrast multilayers and in-plane scattering of 2D photonic crystals. Consider an N-beam TM coplanar diffraction process involving diffraction vectors $\mathbf{g}_0$ ($=\mathbf{0}$), $\mathbf{g}_1, \ldots, \mathbf{g}_{N-1}$ ($N > 1$) that are all parallel to the xz plane in Fig. 1. Based on Eqs. (5), we have $\mathbf{k}_m \cdot \mathbf{k}_n = k_{mx}k_{nx} + g_{mz}g_{nz} + (g_{mz} + g_{nz})p + p^2$. Then, Eqs. (26) for the N-beam case can again be written as an eigenvalue equation,

$$(p^2\boldsymbol{I} - p\boldsymbol{V}^{\pi} + \boldsymbol{U}^{\pi})\underline{\mathbf{H}} = \mathbf{0}, \tag{31}$$

with $\underline{\mathbf{H}} = (H_0, H_1, \ldots, H_{N-1})^T$, which is similar to Eq. (19) except that here matrix $\boldsymbol{V}^{\pi}$ with elements $V^{\pi}_{m,n} = -\zeta_{m-n}(g_{mz} + g_{nz})$ is not a diagonal matrix. The elements of matrix $\boldsymbol{U}^{\pi}$ are $U^{\pi}_{m,n} = \zeta_{m-n}(k_{mx}k_{nx} + g_{mz}g_{nz}) - K^2\delta_{mn}$, where δ_{mn} is the Kronecker δ ($\delta_{mn} = 0$ for $m \neq n$ and $\delta_{mm} = 1$). Similar to Eqs. (19) and (20), Eq. (31) can give $2N$ sets of eigenvalues p_ι and eigenvectors $\underline{\mathbf{H}}^{(\iota)}$ (for $\iota = 1,2,\ldots,2N$). Afterwards, one may derive the internal electric fields from Eq. (30) and use the boundary conditions to determine the strengths of the eigenvectors and the external wave amplitudes. Similar to TE polarization, wave merging occurs when different diffraction vectors have the same tangential components.

For 1D grating structures with $\varphi = 90^\circ$ (Fig. 1), we have $g_{mz} \equiv 0$ and $\boldsymbol{V}^{\pi} = \boldsymbol{O}$. Then Eq. (31) is simplified to a standard eigenvalue equation

$$(p^2\boldsymbol{I} + \boldsymbol{U}^{\pi})\underline{\mathbf{H}} = \mathbf{0} \tag{32}$$

about p^2. Although this equation has the same form as Eq. (21), numerical computations of TM-polarization diffraction of high-contrast gratings (particularly metallic gratings) usually converge much slower than that of TE polarization (thus requiring a large number of diffraction orders). Due to this problem, the TM case has been extensively studied in the literature with various improved algorithms (see, e.g., [5,21,22]), but Eq. (32) remains the fundamental equation. The intense studies of metallic gratings for TM polarization have been motivated also by a variety of novel fascinating plasmonic properties of the gratings found in recent years [11,12,23–25].

IV. GENERAL N-BEAM DIFFRACTION FOR 2D AND 3D PERIODIC STRUCTURES

To model general N-beam diffraction from 3D (photonic) crystals, let us consider the diffraction vector $\mathbf{g}$ in Fig. 1 as any of the involved diffraction vectors $\mathbf{g}_m$ ($m \neq 0$), but $\mathbf{g}_m$ is not necessarily parallel to the xz plane. We write the incident wave as $\tilde{\mathbf{H}}^I \exp(-i\mathbf{K}_0 \cdot \mathbf{r})$ (with $\mathbf{K}_0 \cdot \tilde{\mathbf{H}}^I = 0$). The external diffracted waves corresponding to each diffraction vector $\mathbf{g}_m$ are $\tilde{\mathbf{H}}^R_m \exp(-i\mathbf{K}^R_m \cdot \mathbf{r})$ and $\tilde{\mathbf{H}}^T_m \exp(-i\mathbf{K}^T_m \cdot \mathbf{r})$ above and below the plate, respectively, where $m = 0,1,\ldots,N-1$ and $\mathbf{g}_0 = \mathbf{0}$. Here all the external wave vectors have the same magnitude, $K = 2\pi/\lambda$. We write the internal waves as $\mathbf{H}_m \exp(-i\mathbf{k}_m \cdot \mathbf{r})$, where $\mathbf{k}_m = \mathbf{k}_0 + \mathbf{g}_m$, $\mathbf{k}_0 = k_{0x}\hat{\mathbf{x}} + k_{0y}\hat{\mathbf{y}} + p\hat{\mathbf{z}}$, and p is to be determined. Based on the continuity of the tangential wave-vector components across the surfaces, we have

$$\begin{aligned} \mathbf{k}_m &= k_{mx}\hat{\mathbf{x}} + k_{my}\hat{\mathbf{y}} + (p + g_{mz})\hat{\mathbf{z}}, \\ k_{mx} &= K^T_{mx} = K^R_{mx} = K_{0x} + g_{mx}, \\ k_{my} &= K^T_{my} = K^R_{my} = K_{0y} + g_{my}, \end{aligned}$$

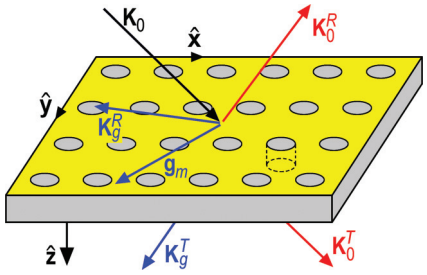

FIG. 5. (Color online) Out-of-plane diffraction from the 2D photonic crystal (invariant with z). All the diffraction vectors $\mathbf{g}_m$ are parallel to the xy plane, but the incident wave vector $\mathbf{K}_0$ has an out-of-plane component, $K_{0z} \neq 0$.

$$K^T_{mz} = -K^R_{mz} = \begin{cases} \sqrt{\Delta_m} & \text{if } \Delta_m \geqslant 0 \\ -i\sqrt{-\Delta_m} & \text{otherwise,} \end{cases} \tag{33}$$

where $\Delta_m = K^2 - k^2_{mx} - k^2_{my}$. Here, if two different diffraction vectors satisfy $g_{mx} = g_{nx}$ and $g_{my} = g_{ny}$ (but with $g_{mz} \neq g_{nz}$), we have $\mathbf{K}^{R,T}_m = \mathbf{K}^{R,T}_n$, which corresponds to wave merging.

Next, inserting the 3D Fourier expansion $\mathbf{H}(\mathbf{r}) = \sum \mathbf{H}_m \exp(-i\mathbf{k}_m \cdot \mathbf{r})$ and Eq. (24) into Eq. (22) leads to the general coupled-wave equations

$$K^2\mathbf{H}_m = -\sum_n \zeta_{m-n}\mathbf{k}_m \times (\mathbf{k}_n \times \mathbf{H}_n). \tag{34}$$

These are vector equations, so we can project each of them onto the x, y, and z axes to obtain three scalar equations. However, it can be strictly proved that *only two of the three scalar equations are independent* due to the transversality condition $\mathbf{k}_m \cdot \mathbf{H}_m = 0$.

A simplified case of general N-beam diffraction is the out-of-plane diffraction from 2D photonic crystals shown in Fig. 5 [26], where the diffraction vectors are always parallel to the xy plane, i.e., they all satisfy $g_{mz} = 0$ and $k_{mz} = p$. Under this condition, projecting Eq. (34) onto the x and y axes and replacing H_{mz} with $-(k_{mx}H_{mx} + k_{my}H_{my})/p$, one can find that the terms p in the denominators are automatically canceled by the corresponding numerators. Then we directly obtain a standard eigenvalue equation

$$(p^2\boldsymbol{W} + \boldsymbol{U})\underline{\mathbf{H}} = \mathbf{0} \tag{35}$$

about p^2, where $\underline{\mathbf{H}} = (H_{0x}, H_{0y}, H_{1x}, H_{1y}, \ldots, H_{N-1,x}, H_{N-1,y})^T$ and $\boldsymbol{W}$ is a $2N \times 2N$ matrix with elements

$$\begin{aligned} W_{2m,2n} &= W_{2m+1,2n+1} = \zeta_{m-n}, \\ W_{2m,2n+1} &= W_{2m+1,2n} = 0. \end{aligned} \tag{36}$$

The elements of matrix $\boldsymbol{U}$ are

$$\begin{aligned} U_{2m,2n} &= \zeta_{m-n}\left(k_{my}k_{ny} + k^2_{nx}\right) - K^2\delta_{mn}, \\ U_{2m,2n+1} &= \zeta_{m-n}(-k_{my}k_{nx} + k_{nx}k_{ny}), \\ U_{2m+1,2n} &= \zeta_{m-n}(-k_{mx}k_{ny} + k_{nx}k_{ny}), \\ U_{2m+1,2n+1} &= \zeta_{m-n}\left(k_{mx}k_{nx} + k^2_{ny}\right) - K^2\delta_{mn}. \end{aligned} \tag{37}$$

Here it is worth emphasizing that $\boldsymbol{W}$ and $\boldsymbol{U}$ are $2N \times 2N$ matrices, compared with the $N \times N$ matrices in Eqs. (21) and (32). Now from Eq. (35) we can obtain $4N$ sets of eigenvalues p_ι and eigenvectors $\underline{\mathbf{H}}^{(\iota)}$ ($\iota = 1,2,\ldots,4N$). For each

eigenvector, the corresponding p_ι then completely determines the internal wave vectors from Eq. (33). The magnetic field of each internal wave is $\mathbf{H}_m^{(\iota)} = H_{mx}^{(\iota)}\hat{\mathbf{x}} + H_{my}^{(\iota)}\hat{\mathbf{y}} - \hat{\mathbf{z}}(k_{mx}H_{mx}^{(\iota)} + k_{my}H_{my}^{(\iota)})/p_\iota$. The electric fields of each eigenmode must be derived from Eq. (30). Subsequently, the eigenmode strengths and the external wave amplitudes $\tilde{H}_{mx}^{R,T}$ and $\tilde{H}_{my}^{R,T}$ can be calculated from $8N$ boundary equations about the continuity of the magnetic and electric vectors along the x and y axes. Afterwards, the z components of the external waves are $\tilde{H}_{mz}^{R,T} = -(K_{mx}^{R,T}\tilde{H}_{mx}^{R,T} + K_{my}^{R,T}\tilde{H}_{my}^{R,T})/K_{mz}^{R,T}$. By setting $|\tilde{\mathbf{H}}^I| = 1$, one finally obtains the diffraction efficiency values of each diffraction order (with $\Delta_m = K^2 - k_{mx}^2 - k_{my}^2 > 0$): $R_m = (K_{mz}^T/K_{0z})(|\tilde{H}_{mx}^R|^2 + |\tilde{H}_{my}^R|^2 + |\tilde{H}_{mz}^R|^2)$ and $T_m = (K_{mz}^T/K_{0z})(|\tilde{H}_{mx}^T|^2 + |\tilde{H}_{my}^T|^2 + |\tilde{H}_{mz}^T|^2)$.

Out-of-plane diffraction of 2D crystals in Fig. 5 does not have the wave merging problem in Sec. II B since different diffraction vectors always have different in-plane components. [This is also true for 1D gratings where Eq. (21) or (32) applies.] Hence, the above mathematical treatments are rigorous and complete. Apparently, they also apply to noncoplanar (conical) diffraction of 1D gratings [4].

For N-beam diffraction from 3D periodic structures, one might choose the projections of Eq. (34) onto the y and z axes and replace H_{mx} with $-(k_{my}H_{my} + k_{mz}H_{mz})/k_{mx}$ to obtain $2N$ scalar equations. These equations can be written as a quadratic eigenequation similar to Eq. (31), but it is obvious that this simple method fails when $k_{mx} \to 0$. To avoid this problem, we use the following method that is similar to the one developed by Stetsko and Chang for treating the **E** fields in x-ray multiple-beam diffraction [8]. We project Eq. (34) onto the x and y axes to obtain $2N$ scalar equations that can be represented by two matrix equations:

$$(\boldsymbol{Q}_z\boldsymbol{F}\boldsymbol{Q}_z + \boldsymbol{S}_{yy})\underline{\mathbf{H}}^x + \boldsymbol{S}_{yx}\underline{\mathbf{H}}^y - \boldsymbol{Q}_z\boldsymbol{F}\boldsymbol{Q}_x\underline{\mathbf{H}}^z = \mathbf{0}, \quad (38)$$

$$\boldsymbol{S}_{xy}\underline{\mathbf{H}}^x + (\boldsymbol{Q}_z\boldsymbol{F}\boldsymbol{Q}_z + \boldsymbol{S}_{xx})\underline{\mathbf{H}}^y - \boldsymbol{Q}_z\boldsymbol{F}\boldsymbol{Q}_y\underline{\mathbf{H}}^z = \mathbf{0}, \quad (39)$$

where $\underline{\mathbf{H}}^x = (H_{0x}, H_{1x}, \ldots, H_{N-1,x})^T$, $\underline{\mathbf{H}}^y = (H_{0y}, H_{1y}, \ldots, H_{N-1,y})^T$, and $\underline{\mathbf{H}}^z = (H_{0z}, H_{1z}, \ldots, H_{N-1,z})^T$. All the other symbols in Eqs. (38) and (39) are $N \times N$ matrices, among which $\boldsymbol{Q}^x$, $\boldsymbol{Q}^y$, and $\boldsymbol{Q}^z$ are diagonal matrices with diagonal elements $Q_x^{m,m} = k_{mx}$, $Q_y^{m,m} = k_{my}$, and $Q_z^{m,m} = k_{mz}$, respectively. The elements of the other matrices are $F_{m,n} = \zeta_{m-n}$, $S_{xx}^{m,n} = \zeta_{m-n}k_{mx}k_{nx} - K^2\delta_{mn}$, $S_{yy}^{m,n} = \zeta_{m-n}k_{my}k_{ny} - K^2\delta_{mn}$, $S_{xy}^{m,n} = -\zeta_{m-n}k_{mx}k_{ny}$, and $S_{yx}^{m,n} = -\zeta_{m-n}k_{my}k_{nx}$.

Now we introduce two new variables,

$$\underline{\mathbf{h}}^\alpha = \boldsymbol{F}\boldsymbol{Q}_z\underline{\mathbf{H}}^x - \boldsymbol{F}\boldsymbol{Q}_x\underline{\mathbf{H}}^z, \quad (40)$$

$$\underline{\mathbf{h}}^\beta = \boldsymbol{F}\boldsymbol{Q}_z\underline{\mathbf{H}}^y - \boldsymbol{F}\boldsymbol{Q}_y\underline{\mathbf{H}}^z, \quad (41)$$

based on which Eqs. (38) and (39) become

$$\boldsymbol{Q}_z\underline{\mathbf{h}}^\alpha + \boldsymbol{S}_{yy}\underline{\mathbf{H}}^x + \boldsymbol{S}_{yx}\underline{\mathbf{H}}^y = \mathbf{0}, \quad (42)$$

$$\boldsymbol{Q}_z\underline{\mathbf{h}}^\beta + \boldsymbol{S}_{xy}\underline{\mathbf{H}}^x + \boldsymbol{S}_{xx}\underline{\mathbf{H}}^y = \mathbf{0}. \quad (43)$$

The matrix equation corresponding to the projections of Eq. (34) onto the z axis is $-\boldsymbol{Q}_x\boldsymbol{F}\boldsymbol{Q}_z\underline{\mathbf{H}}^x - \boldsymbol{Q}_y\boldsymbol{F}\boldsymbol{Q}_z\underline{\mathbf{H}}^y + (\boldsymbol{S}_{xx} + \boldsymbol{S}_{yy} + K^2\boldsymbol{I})\underline{\mathbf{H}}^z = \mathbf{0}$, which is a linear combination of Eqs. (38) and (39). We write this equation here for convenience to eliminate $\underline{\mathbf{H}}^z$ in Eqs. (40) and (41), which can be realized by adding the product of $\boldsymbol{Q}_x$ and Eq. (40) and the product of $\boldsymbol{Q}_y$ and Eq. (41) to this equation. Then we obtain

$$\underline{\mathbf{H}}^z = -K^{-2}(\boldsymbol{Q}_x\underline{\mathbf{h}}^\alpha + \boldsymbol{Q}_y\underline{\mathbf{h}}^\beta), \quad (44)$$

based on which Eqs. (40) and (41) can be rewritten as

$$\left(K^{-2}\boldsymbol{Q}_x^2 - \boldsymbol{F}^{-1}\right)\underline{\mathbf{h}}^\alpha + K^{-2}\boldsymbol{Q}_x\boldsymbol{Q}_y\underline{\mathbf{h}}^\beta + \boldsymbol{Q}_z\underline{\mathbf{H}}^x = \mathbf{0}, \quad (45)$$

$$K^{-2}\boldsymbol{Q}_x\boldsymbol{Q}_y\underline{\mathbf{h}}^\alpha + \left(K^{-2}\boldsymbol{Q}_y^2 - \boldsymbol{F}^{-1}\right)\underline{\mathbf{h}}^\beta + \boldsymbol{Q}_z\underline{\mathbf{H}}^y = \mathbf{0}. \quad (46)$$

In terms of $k_{mz} = g_{mz} + p$, Eqs. (42), (43), (45), and (46) can be written as a $4N \times 4N$ eigenvalue equation

$$(p\boldsymbol{I}_{4N} + \boldsymbol{U}_{4N})\underline{\mathbf{H}}_{4N} = \mathbf{0}, \quad (47)$$

where $\underline{\mathbf{H}}_{4N} = (\underline{\mathbf{h}}^\alpha, \underline{\mathbf{h}}^\beta, \underline{\mathbf{H}}^x, \underline{\mathbf{H}}^y)^T$, $\boldsymbol{I}_{4N}$ is the $4N \times 4N$ identity matrix, and

$$\boldsymbol{U}_{4N} = \begin{pmatrix} \boldsymbol{G}_z & \boldsymbol{O} & \boldsymbol{S}_{yy} & \boldsymbol{S}_{yx} \\ \boldsymbol{O} & \boldsymbol{G}_z & \boldsymbol{S}_{xy} & \boldsymbol{S}_{xx} \\ K^{-2}\boldsymbol{Q}_x^2 - \boldsymbol{F}^{-1} & K^{-2}\boldsymbol{Q}_x\boldsymbol{Q}_y & \boldsymbol{G}_z & \boldsymbol{O} \\ K^{-2}\boldsymbol{Q}_x\boldsymbol{Q}_y & K^{-2}\boldsymbol{Q}_y^2 - \boldsymbol{F}^{-1} & \boldsymbol{O} & \boldsymbol{G}_z \end{pmatrix}. \quad (48)$$

Here, $\boldsymbol{G}_z$ is a diagonal matrix with $G_z^{m,m} = g_{mz}$ (for $m = 0,1,\ldots,N-1$), and $\boldsymbol{O}$ is the $N \times N$ null matrix. Note that the elements of $\boldsymbol{F}^{-1}$ are actually $F_{m,n}^{-1} = \epsilon_{m-n}$ that can also be directly calculated from Eq. (9) without matrix inversion [5]. Equation (47) gives $4N$ sets of eigenvalues p_ι and eigenvectors $\underline{\mathbf{H}}_{4N}^{(\iota)}$ (for $\iota = 1,2,\ldots,4N-1$), but we are only interested in the components $H_{mx}^{(\iota)}$ and $H_{my}^{(\iota)}$ (for $m = 0,1,\ldots,N-1$) since the z components of the magnetic fields may be obtained from $H_{mz}^{(\iota)} = -(k_{mx}H_{mx}^{(\iota)} + k_{my}H_{my}^{(\iota)})/(p_\iota + g_{mz})$ due to $\mathbf{k}_m^{(\iota)} \cdot \mathbf{H}_m^{(\iota)} = 0$. [Equivalently, one may use Eq. (44) to calculate $H_{mz}^{(\iota)}$.] Afterwards, the treatments of the $8N$ boundary-condition equations are similar to those of out-of-plane diffraction from 2D crystals.

The above formulas are strictly valid (without singularities) for both multiple-beam x-ray crystal diffraction and 3D photonic crystal diffraction except that the convergence of the latter could be slow for high-contrast structures. In addition, wave merging can occur in photonic crystal diffraction if any two of the involved diffraction vectors have the same tangential components. This should be specifically treated, although it is generally unnecessary for x-ray diffraction.

V. DISCUSSION AND CONCLUSION

We have reformulated the conventional x-ray dynamical theory and coupled-wave theory into a universal FCWDT, of which the fundamental coupled-wave equations for almost all practical diffraction geometry can always be written as a simple and straightforward eigenvalue equation that may be solved by standard mathematical procedures. The FCWDT also removes almost all the approximations, misconceptions or mistakes (e.g., the wave merging problem), and the extreme complications of various conventional coupled-wave theories (as well as x-ray dynamical theories) in the related large literature. Therefore, the FCWDT described in this paper is rigorous and, at the same time, easily understandable even for beginners. It can be applied to diffraction and/or scattering of electromagnetic waves from all kinds of (nonmagnetic)

periodic structures, including x-ray diffraction from crystals and soft x-ray and long-wavelength light diffraction from periodic multilayers, gratings (including nonplanar gratings with arbitrary surface profiles; see Fig. 3), and photonic crystals.

The diffraction of electromagnetic waves from periodic structures is rich in physics and, at the same time, is of practical importance. Due to the difficulties and complexities of mathematical analyses and numerical computations, only a limited number of specific diffraction cases have been studied in the literature, while numerous mechanisms and the associated applications remain unexplored. Here the universal FCWDT may help improve this situation. For periodic structures with relative low permittivity contrast, such as dielectric photonic crystals, the FCWDT formulation can be readily used for fast computation of their optical and diffraction properties. In general, retaining only a few tens of diffraction orders can achieve high-resolution convergence for dielectric structures. Note that for dispersive media, the absorption is included in the *complex* permittivity. Therefore, the FCWDT can automatically treat absorption and resonant (anomalous) diffraction. For instance, the Borrmann effect is a very famous example of two-beam diffraction [2], which is naturally included in the formulas of Secs. II A and III A. For highly conducting metallic structures, however, the magnitude of the complex permittivity ε can be extremely large for long-wavelength electromagnetic waves. Consequently, the numerical convergence could be very slow or difficult, particularly for 2D and 3D metallic structures. Fortunately, the FCWDT is scalable to include an extremely large number of diffraction orders so as to achieve, in principle, any desired resolution. We have tested that in most cases, retaining tens of thousands of diffraction orders in FCWDT (which requires large computer memory and computing time) does not cause noticeable numerical instability. Under this condition, convergence of many metallic structures can be reasonably achieved. On the other hand, the algorithms can be improved by matrix manipulation and optimization or other methods, similar to TM-polarization diffraction of 1D gratings [5,22], to reach the same resolution with less diffraction orders and computing time.

In fact, light scattering from metallic nano- or microstructures (e.g., plasmonic materials [25] and metamaterials [27]) has become a fascinating new frontier of science and technology in recent years. Complete understanding of the optical properties and mechanisms of these novel materials requires significant efforts to develop or improve the computing algorithms and techniques. The FCWDT provides the fundamental principles and formulas, based on which such developments and improvements are possible. Once the convergence problem is solved, the FCWDT in general can give much more reliable and accurate results than other commonly used computing techniques (such as the finite-difference time-domain method [28]). Therefore, it is expected to have a wide range of applications for exploration, modeling, design, and analyses of novel optical devices.

ACKNOWLEDGMENTS

This work was supported by the US Department of Energy, Office of Science, Office of Basic Energy Sciences, under Contract No. DE-AC-02-06CH11357. R.W.P. was supported by the Ministry of Science and Technology of China (Grants No. 2012CB921502 and No. 2010CB630705), by the NSFC (Grants No. 11034005, No. 61077023, and No. 11021403), and partly by the Ministry of Education of China (Grant No. 20100091110029). M.G.H. thanks CNPq/PQ (Grant No. 305034/2010-3) for financial support.

[1] Z. G. Pinsker, *Dynamical Scattering of X-Rays in Crystals* (Springer-Verlag, Berlin, 1978).
[2] A. Authier, *Dynamical Theory of X-ray Diffraction* (Oxford University Press, New York, 2001).
[3] M. G. Moharam and T. K. Gaylord, J. Opt. Soc. Am. **71**, 811 (1981).
[4] M. G. Moharam, E. B. Grann, D. A. Pommet, and T. K. Gaylord, J. Opt. Soc. Am. A **12**, 1068 (1995).
[5] P. Lalanne and G. M. Morris, J. Opt. Soc. Am. A **13**, 779 (1996).
[6] M. Nevière and E. Popov, *Light Propagation in Periodic Media: Diffraction Theory and Design* (Marcel Dekker, New York, 2003).
[7] R. Colella, Acta Crystallogr. A **30**, 413 (1974).
[8] Y. P. Stetsko and S.-L. Chang, Acta Crystallogr. A **53**, 28 (1997).
[9] S. Bajt, H. N. Chapman, A. Aquila, and E. Gullikson, J. Opt. Soc. Am. A **29**, 216 (2012).
[10] X. Huang and M. Dudley, Acta. Crystallogr. A **59**, 163 (2003).
[11] X.-R. Huang and R.-W. Peng, J. Opt. Soc. Am. A **27**, 718 (2010).
[12] X.-R. Huang, R.-W. Peng, and R.-H. Fan, Phys. Rev. Lett. **105**, 243901 (2010).
[13] L. G. Parratt, Phys. Rev. **95**, 359 (1954)
[14] M. Born and E. Wolf, *Principles of Opitcs*, 7th ed. (Cambridge University Press, New York, 2002).
[15] X.-R. Huang, J. Synchrotron Rad. **18**, 899 (2011).
[16] M. G. Moharam and T. K. Gaylord, J. Opt. Soc. Am. **73**, 1105 (1983).
[17] M. G. Moharam, D. A. Pommet, E. B. Grann, and T. K. Gaylord, J. Opt. Soc. Am. A **12**, 1077 (1995).
[18] L. Li, J. Opt. Soc. Am. A **10**, 2581 (1993).
[19] M. Pisarenco, J. Maubach, I. Setija, and R. Mattheij, J. Opt. Soc. Am. A **28**, 1364 (2011).
[20] W. Cho, X. Huang, and M. Dudley, Acta Crystallogr. A **60**, 195 (2004).
[21] E. Popov, B. Chernov, M. Nevière, and N. Bonod, J. Opt. Soc. Am. A **21**, 199 (2004).
[22] B. Guizal, H. Yala, and D. Felbacq, Opt. Lett. **34**, 2790 (2009).
[23] X. R. Huang, R. W. Peng, Z. Wang, F. Gao, and S. S. Jiang, Phys. Rev. A **76**, 035802 (2007).
[24] R.-H. Fan, R.-W. Peng, X.-R. Huang, J. Li, Y. Liu, Q. Hu, M. Wang, and X. Zhang, Adv. Mater. **24**, 1980 (2012).
[25] F. J. Garcia-Vidal, L. Martin-Moreno, T. W. Ebbesen, and L. Kuipers, Rev. Mod. Phys. **82**, 729 (2010).
[26] L. Li, J. Opt. Soc. Am. A **14**, 2758 (1997).
[27] Y. Liu and X. Zhang, Chem. Soc. Rev. **40**, 2494 (2011).
[28] A. Taflove and S. C. Hagness, *Computational Electrodynamics: The Finite-Difference Time-Domain Method*, 3rd ed. (Artech, Norwood, 2005).